An unexpected hardening behaviour of carbon-fiber epoxy composites under flexural fatigue loading and its intensification by graphene nano-fillers

Alok K. Srivastava[a], Aparna Singh[b*]

[a] Centre for Research in Nanotechnology & Science, Indian Institute of Technology Bombay, Mumbai 400076, India

[b] Department of Metallurgical Engineering and Materials Science, Indian Institute of Technology Bombay, Mumbai 400076, India

Abstract

The fatigue performance of carbon fiber reinforced polymer (CFRP) composites under cyclic loading remains a significant concern in various engineering applications due to the complex damage mechanisms and uncertain failure modes associated with these materials. Despite their exceptional strength-to-weight ratio, CFRP composites are prone to progressive damage accumulation, leading to premature failure and reduced structural integrity. The present study investigates the flexural fatigue response of pristine CFRPs and CFRPs with added graphene nanoplatelets (GNPs), accompanied by in-situ microscopy for progressive damage analysis. Eight layers of carbon fibers fabric, both pristine and GNP coated were utilized to fabricate the composites using vacuum-assisted resin transfer molding (VARTM) technique. GNP-added composites exhibited significantly improved monotonic flexural and fatigue life compared to pristine composites. The dissipated strain energy density (DSED) with number of cycles was also monitored as a function of cycles and correlated with the damage happening in the composite using in-situ optical imaging. While cycling at or below three-quarters of the maximum tensile stress, it was observed

*Corresponding author. E-mail address: aparna_s@iitb.ac.in (Aparna Singh), Tel: +91-22-2576-7605

that the DSED decreased with the number of cycles in both composites. However, at higher loads, the DSED was found to increase progressively, ultimately shooting up during catastrophic failure.These composites that showed a decrease in DSED with cycles, did not fail even at one million cycles and had a higher residual strength than the original when they were forced to break under monotonic loading and the percentage increment was even higher when GNPs were used. Additionally, post-failure fracture surface examination using scanning electron microscopy (SEM) was conducted to understand the influence of GNP addition on damage evolution of CFRPs.

Keywords: Hardening, Carbon fiber, Graphene nanoplatelets, Fatigue, Damage evolution, VARTM

1. Introduction

Carbon fiber reinforced polymer (CFRP) composites are known for their superior strength-to-weight ratio; however, they have an inherent non-uniform structure that makes them vulnerable to failure due to the formation of delamination between different layers or the occurrence of micro-cracks at the interface between the reinforced fibers and the matrix, especially when subjected to repeated cyclic loading [1]. Various studies have investigated the mechanical properties of the composite after incorporation of nanofillers such as carbon black, nano-silica particles, carbon nanotubes, and graphene oxides into epoxy matrix [2–5]. These studies have observed an enhancement in both the strength and stiffness of the resulting composites. On the other hand, it is possible to selectively strengthen the interface or interphase between carbon fibers and epoxy by coating the carbon fibers with nanofillers

using various coating techniques such as solvent spraying, layer by layer coating and electrophoretic deposition [6–9]. Various studies have observed that reinforcing the interphase through nano-fillers leads to enhancement in the interlaminar shear strength [6,10], tensile strength [7,8,11,12], flexural strength [7,9,13,14], fracture toughness [7,15] and wear resistance [16].

By incorporating 0.1 wt.% of GNP in CFRPs using a 3-roll high shear mixture and subsequent hand layup and compression mold processes of 10-layer woven carbon fabrics, a significant improvement in flexural fatigue life of up to 155% has been achieved, as reported by Tareq et al. [17]. The presence of strongly bonded fibers in GNP-added CFRPs has been observed in post-fracture surfaces, highlighting a distinct difference when compared to CFRPs without GNP. A different study compared the flexural fatigue life of various CFRP laminates with different mixing ratios of multi-walled carbon nanotubes (MWCNTs) and GNPs in epoxy [18]. To create these laminates, fourteen layers of unidirectional carbon fiber epoxy were made using hand layup and subsequent hot-pressing processes. The study reported an improvement of 9.3% and 11% in monotonic flexural strength and fatigue limit, respectively, for the laminates that were modified with a nanofiller ratio of 9:1 (MWCNT:GNP). SEM fractographs have shown fiber-matrix debonding, MWCNT pull-outs and crack deflection. In a study conducted by Shen et al. [19], the tension fatigue life of CFRPs was enhanced by 37 times when 0.25 wt.% of GNPs-mixed epoxy was used to manufacture the laminates through hot compression molding. Another study compared the tension fatigue life of CFRPs that were modified with MWCNT and a few-layered graphene (FLG) was added to the epoxy and the

laminates were produced through hot press molding [20]. The study reported a maximum improvement of 5- and 15-fold in the tension fatigue life of the MWCNT and FLG modified CFRPs respectively. A thorough post fracture microscopic investigation unveiled nanoparticle-matrix debonding, growth of plastic voids, nanotube pull-out and the presence of thin and creased FLG-nanoparticles in close proximity to the carbon fiber.

Previous studies conducted by authors have demonstrated that the spray coating of graphene nanoplates (GNPs) onto carbon fibers, followed by the manufacturing of composites through vacuum-assisted resin transfer molding (VARTM) leads to enhanced mechanical properties [12–14,21]. However, to date, no studies have been found that examine the fatigue performance of such composites. Moreover, the existing literature has not thoroughly investigated the progression of damage and failure mechanisms in pristine CFRPs and CFRPs incorporated with GNPs under cyclic bending fatigue conditions. In this study, GNP/CF/epoxy composites were manufactured by initially spray coating the carbon fibers with GNPs, followed by the fabrication of composites using vacuum-assisted resin transfer molding (VARTM) technique. These composites were subjected to monotonic and cyclic bending loading conditions. Furthermore, an in-situ examination of crack initiation and propagation during flexural fatigue of the CFRPs was performed using an optical microscope. The study also included an monitoring of damage evolution by measuring dissipated strain energy density (DSED) throughout the fatigue cycles. Additionally, the residual flexural strength of the composites that remained intact after undergoing one million cycles was also investigated. Post-failure fracture surface examination using

scanning electron microscopy (SEM) was conducted to gain insights into the influence of GNP addition on damage evolution in CFRPs.

2. Experimental procedures

2.1 Materials

Uni-directional 2 × 2 twill woven carbon fiber (polyacrylonitrile based), graphene nanoplatelets (GNPs) and an epoxy resin were used in the study. Carbon fiber filaments coated with epoxy-compatible sizing were purchased from Bhor Chemicals and Plastics Pvt. Ltd., Mumbai, India. Tensile strength and elastic modulus of the carbon fiber (CF) were quoted as 4000 MPa and 240 GPa respectively. Carbon fabric was composed of uniform tows made up of carbon fiber filaments with each tow containing 3000 filaments. Each individual filament has a diameter of ~7 μm. Graphene nanoplatelets (purity ~99%) with an average lateral dimension of 5-8 μm and thickness ~2-5 nm was supplied by Ad-Nano Technologies Private Limited, Karnataka, India. The quoted surface area and the number of layers of GNPs were ~380 m^2/g and 2-4 respectively. Laminating grade low viscosity epoxy resin (Epofine-5052) and Finehard-5052 as a hardener was provided by Fine Finish Organics Private Ltd., Mumbai, India. Epoxy resin and hardener were mixed in a ratio of 100:38 by weight as per the manufacturer's datasheet. All the materials were used as received unless otherwise stated.

2.2 Spray coating of GNPs on carbon fibers

The process of spray coating GNPs onto carbon fiber fabrics was carried out using an airbrush system, specifically the Pilot Power AB-15, manufactured by Manik Radiators Pvt.

Ltd. in India. The airbrush system was connected to a high-performance single-piston air compressor. The coating was done with a concentration of 0.4 wt.% in a 0.4GNP laminate. To prepare for the spray coating, perticular weight percentage of GNPs was sonicated in 300 ml of ethanol for 30 minutes using a probe-type sonicator with a frequency of 3 kHz and power of 250 Watts. The resulting GNP-ethanol suspension was filled into the spray gun and then sprayed onto both sides of the carbon fiber fabric in consecutive passes. Each set of laminates included eight fabrics that were spray-coated with a concentration of 0.4 wt.% of GNPs in a 0.4GNP laminate.

2.3 Manufacturing of GNP/CF/epoxy laminates

The vacuum-assisted resin transfer molding (VARTM) technique was used to fabricate the laminates. The process began by stacking eight carbon fabrics on a flat granite table to prepare for vacuum bagging. Peel ply was placed on both sides of the fabric stack and flow mesh was placed on the top side of the fabric stack. Two openings were made using a vacuum cylindrical pipe: one for the inlet of the epoxy-hardener mixture and another for pulling out the air from the bagging. Before infusion, the epoxy-hardener mixture was degassed to remove any air bubbles that might have been trapped during the mixing process. Once the mixture was degassed, the vacuum was initiated through the outlet connected to the vacuum pump, and the resin mixture was infused and passed through the flow mesh. The flow mesh ensured that the resin flowed uniformly in all directions. The laminate was cured in two stages: first, it was cured at ambient temperature for 24 hours, and then it was kept in an oven at 100°C for 2 hours. A control laminate, which had not

undergone any fiber treatment or GNP coating, was named "pristine," while a laminate coated with 0.4 wt.% of GNPs was referred to as a "0.4GNP laminate."

2.4 Testing and characterization

The fatigue test was conducted using an Instron ElectroPuls™ E1000 machine with a 1 kN capacity, at four different stress levels. The test was performed under load control mode at a frequency of 5 Hz. The R-ratio, which is the ratio of the maximum stress to the minimum stress, was kept as +0.1, and the number of cycles to failure was recorded for each stress level. The fractured surfaces of the specimens were examined using a scanning electron microscope (SEM) to understand the failure behavior under cyclic loading. Additionally, in-situ observation during the test was carried out using a stereo microscope to record the events of crack initiation and propagation.

The fractured surfaces of the composite were examined using a Hitachi S-3400 N model scanning electron microscope (SEM) after coating the sample with a few nanometer thin layer of gold.

3. Results and discussions

3.1 Flexural properties

Fig. 1 and Table 1 shows the average values of flexural strength, flexural modulus and flexural strain at maximum flexural stress (failure strain) for both pristine and 0.4GNP laminate. Flexural strength of 0.4GNP laminate shows an approximate increase of 10% compared to pristine laminate. Additionally, failure strain of the 0.4GNP laminate shows an enhancement of approximately 7% when compared to pristine laminate. However, there is

no significant change in the flexural modulus observed between both the laminates. These findings suggest that incorporating 0.4 wt.% GNP coating positively impacts the flexural properties and overall performance of the laminate.

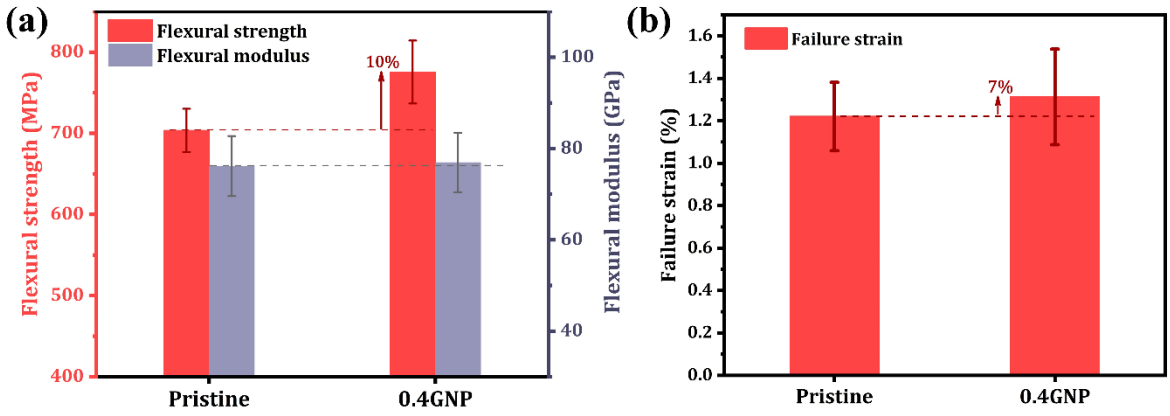

Fig. 1. Flexural properties of pristine and 0.4GNP composites

Table 1 Flexural properties pristine and 0.4GNP composites

Laminate	Flexural strength (MPa)	Flexural modulus (GPa)	Strain at maximum flexural stress (%)
Pristine	703 ± 26	76 ± 6	1.22 ± 0.16
0.4GNP	775 ± 38	77 ± 6	1.31 ± 0.22

3.2 Fatigue test response

Fatigue tests were conducted using bending loads at various stress levels while maintaining a stress ratio (R) of 0.1 and a frequency of 5 Hz. A minimum of three specimens were tested at each stress level, and the obtained results are graphically illustrated in Fig. 2. At

the most elevated stress levels (680 MPa), 0.4GNP laminate exhibited a significantly higher number of cycles to failure, approximately 20 times more, in comparison to the pristine laminate. Furthermore, at a stress level of 640 MPa, 0.4GNP specimen demonstrated approximately 43 times more average cycles to failure compared to pristine laminate. In contrast, at stress levels of 600 MPa and the lowest stress level of 580 MPa, both laminates exhibited a similar number of cycles to failure, and many of the specimens did not fracture and passed the run-out criteria. Therefore, there was no substantial difference observed in the fatigue behavior of the two laminates at these lower stress levels.

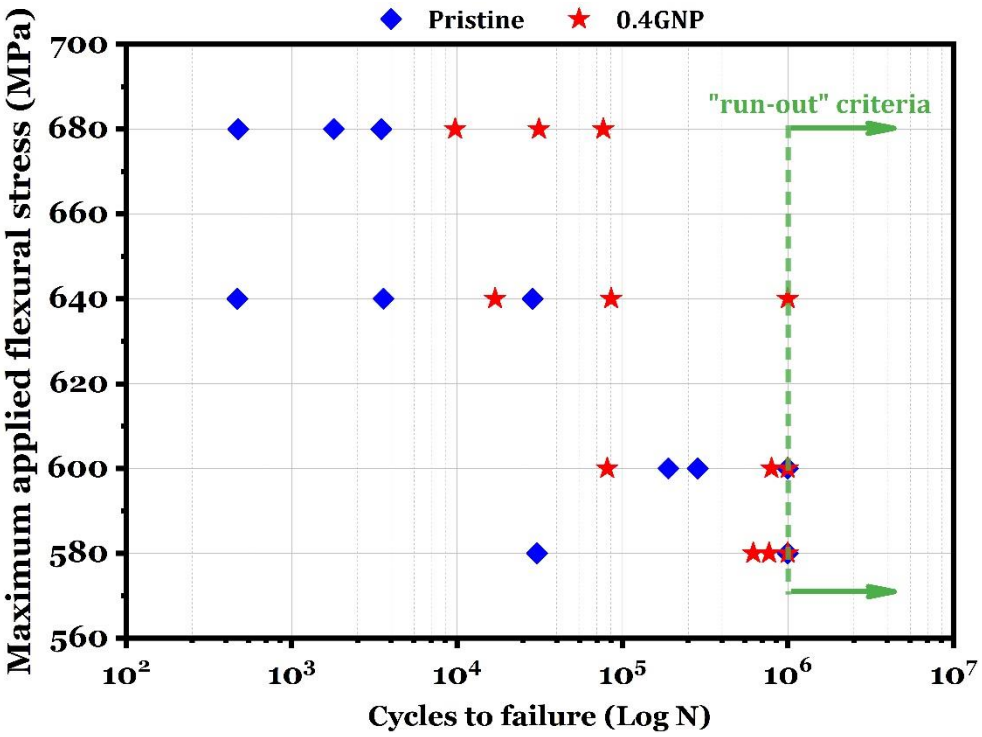

Fig. 2. Fatigue life results of pristine and 0.4GNP composites

3.3 Residual flexural properties

Residual flexural properties of the specimens that did not fracture and met the run-out criteria during fatigue tests were investigated, and the results are presented in Fig. 3. 0.4GNP laminates exhibit a significant increase of 15% and 14% in residual flexural strength and flexural modulus respectively compared to the pristine laminate. However, there is no substantial difference observed in the residual flexural strain for both laminates. It is noteworthy that both pristine and 0.4GNP laminate exhibit an improvement in residual flexural strength of 12% and 17% respectively, when compared to their respective flexural strengths prior to the fatigue test. Moreover, residual failure strains of both laminates are also found to be improved by approximately 10% and 6% respectively. However, there was no improvement observed in the residual flexural modulus of either laminate. In fact, flexural modulus decreased by 9% in the case of pristine laminate.

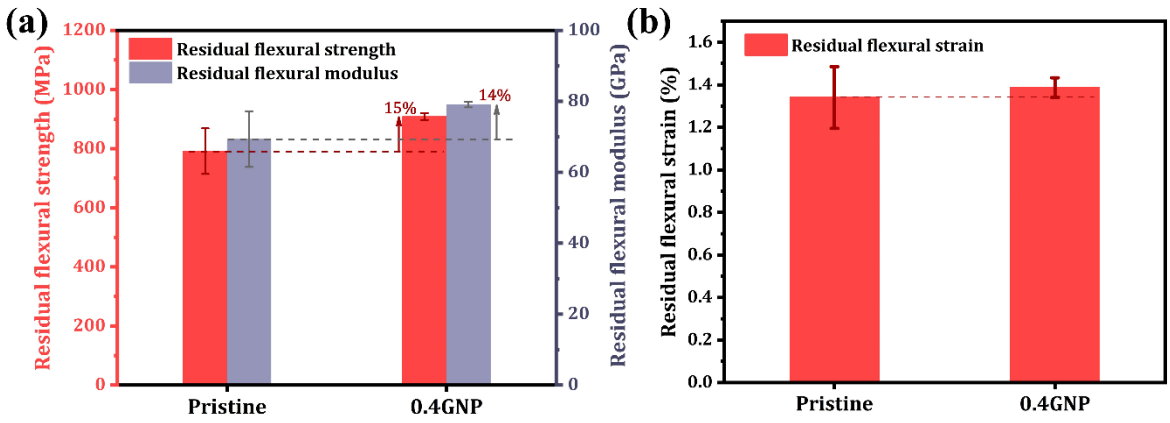

Fig. 3. Residual flexural properties of pristine and 0.4GNP composites

3.4 Hysteresis loop

A hysteresis loop can constructed by plotting the peak and valley values of displacement as along with the load experienced by specimen during the cyclic loading and unloading process. It is a graphical representation used to assess the fatigue damage in FRP (Fiber Reinforced Polymer) composites and is a measure of dissipated strain energy density (DSED) once normalized by the sample volume. This DSED is directly associated with crack growth in FRP composite specimens. Fig. 4 shows the comparison of hysteresis loops between pristine laminate and 0.4GNP laminate at both highest (680 MPa) and lowest (580 MPa) applied stress levels at different number of cycles. Hysteresis loops have been offset along the displacement axis to ensure a clear representation. The DSED of 0.4GNP specimen at 1000 cycles, under a stress level of 680 MPa, was determined to be 23% lower compared to pristine specimen (Fig. 4a). Similarly, at 2000 cycles, DSED of 0.4GNP specimen was found to be ~25% lower than that of pristine specimen. The decrease in DSED for the 0.4GNP laminate compared to the pristine laminate is less significant at a stress level of 580 MPa, with reductions of 6.2% and 5.7% observed at 1000 and 2000 cycles respectively (Fig. 4b). This is in contrast to the results shown in Fig. 4a, where the reduction in DSED is more pronounced at a stress level of 680 MPa.

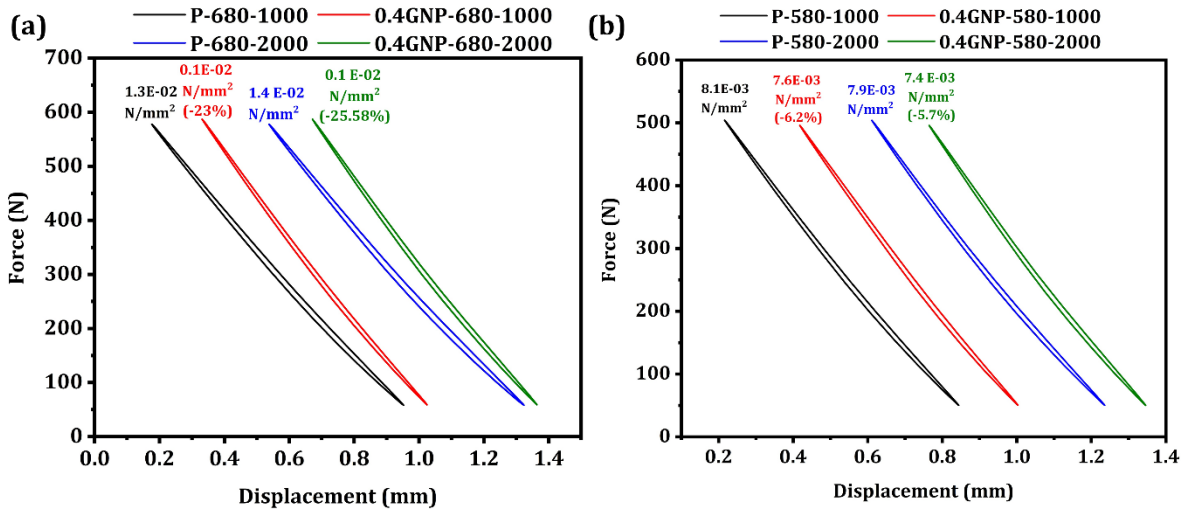

Fig. 4. Hysteresis loop and dissipated strain energy density (DSED) comparison of pristine and 0.4GNP composites at (a) 680 MPa (b) 580 MPa applied flexural stress level at N = 1000 and 2000 cycles

In addition, a detailed analysis of the DSED is conducted by plotting the DSED as a function of the number of cycles for all stress levels (Fig. 5). The DSED of 0.4GNP laminate is consistently lower than that of pristine laminate across all stress levels during the fatigue test (Fig. 5 a, b, c and d). The specimens that failed after a specific number of cycles, particularly at stress levels of 680 MPa and 640 MPa, exhibited enhancement in DSED as the number of cycles progressed (Fig. 5 a and b). Conversely, specimens that did not fail until reaching higher numbers of cycles ($5 \times 10^5 – 1 \times 10^6$) demonstrated a slight decrease in DSED until they approached the point just before final failure (Fig. 5 e and f). In addition, all specimens that were subjected to three distinct stress levels (640 MPa, 600 MPa, and 580 MPa) and met the specified run-out criteria exhibit a gradual reduction in DSED as the number of cycles increases (Fig. 5g). A representation of development of strains measured through DIC in these specimens can be seen in Appendix A.

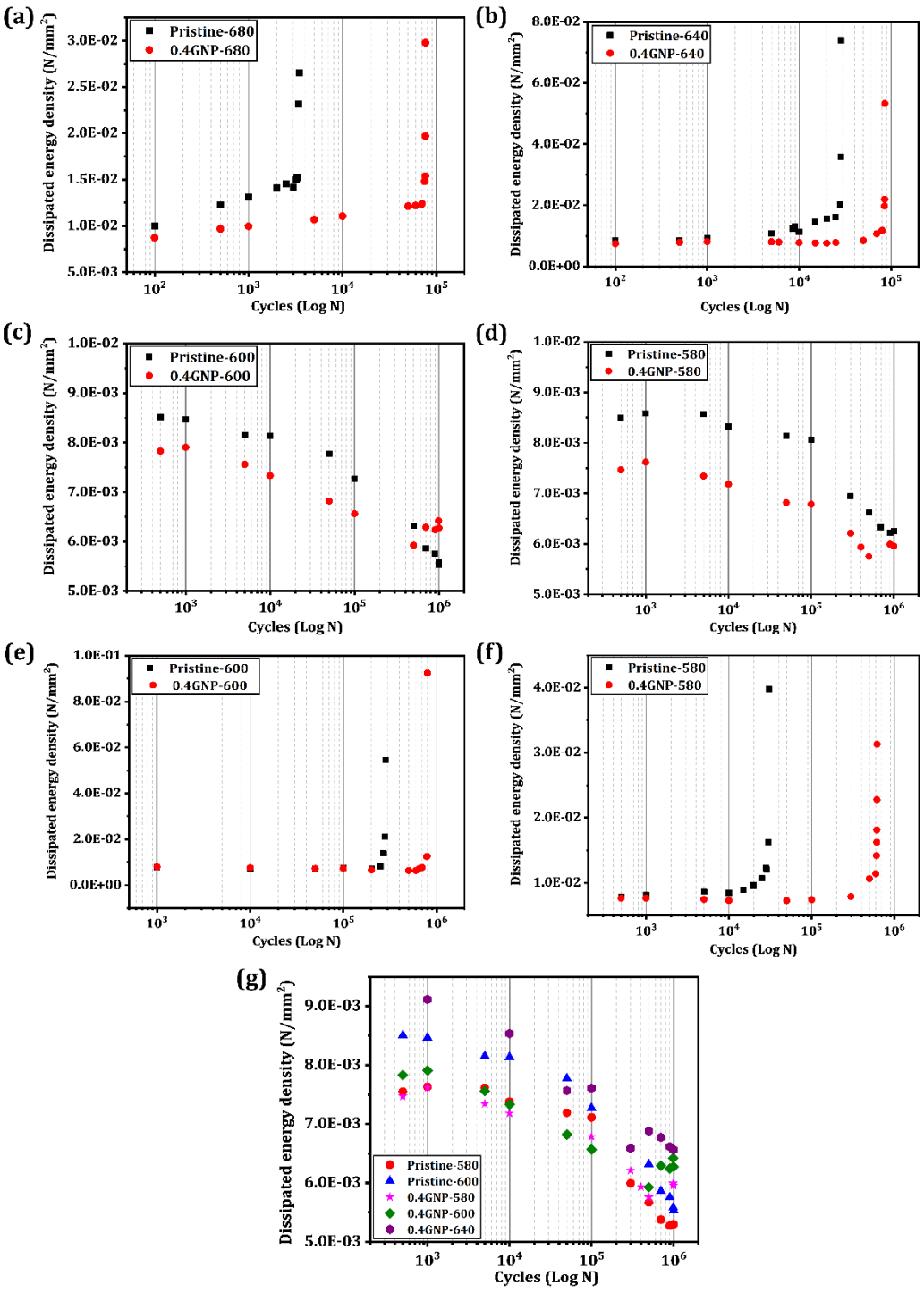
(a)
Pristine-680
0.4GNP-680
Dissipated energy density (N/mm²)
Cycles (Log N)
(b)
Pristine-640
0.4GNP-640
Dissipated energy density (N/mm²)
Cycles (Log N)
(c)
Pristine-600
0.4GNP-600
Dissipated energy density (N/mm²)
Cycles (Log N)
(d)
Pristine-580
0.4GNP-580
Dissipated energy density (N/mm²)
Cycles (Log N)
(e)
Pristine-600
0.4GNP-600
Dissipated energy density (N/mm²)
Cycles (Log N)
(f)
Pristine-580
0.4GNP-580
Dissipated energy density (N/mm²)
Cycles (Log N)
(g)
Pristine-580
Pristine-600
0.4GNP-580
0.4GNP-600
0.4GNP-640
Dissipated energy density (N/mm²)
Cycles (Log N)

Fig. 5. Dissipated strain energy density (DSED) of pristine and 0.4GNP composites at (a) 680 MPa (b) 640 MPa (c,e) 600 MPa and (d,f) 580 MPa applied flexural stress level; (g) plot showing all specimens that met the run-out criteria

3.5 Damage evolution during fatigue loading

An insitu optical microscope was employed to accurately record images at specific cycles for various stress levels throughout the fatigue test. Fig. 6, Fig. 7, Fig. 8 and Fig. 9 exhibit micrographs illustrating the initiation and propagation of cracks during cyclic loading. Additionally, these figures also depict the corresponding plot demonstrating the DSED throughout the test. In the case of pristine specimen subjected to a stress level of 680 MPa, no cracks were observed until 1100 cycles (as depicted in Fig. 6a). Furthermore, associated DSED during this period showed minimal increase. However, an abrupt rise in DSED was observed as the cycle count reached 1280, and this acceleration continued with subsequent increases in the number of cycles. Notably, after 1750 cycles, the formation of an additional crack became evident, leading to a rapid escalation in DSED until the ultimate fracture occurred. In 0.4GNP specimens illustrated in Fig. 6b, first crack occurred within the area of epoxy-rich region or transverse weave thread region after 300 cycles at a stress level of 680 MPa. Following this, there was a slight increase in DSED and the crack gradually propagated until 7000 cycles. This gradual propagation of the crack led to a progressive increase in DSED. However, suddenly, both this ply and another ply below it failed, resulting in delamination and a rapid surge in DSED. Furthermore, DSED kept increasing along with the formation of a new crack after 9100 cycles.

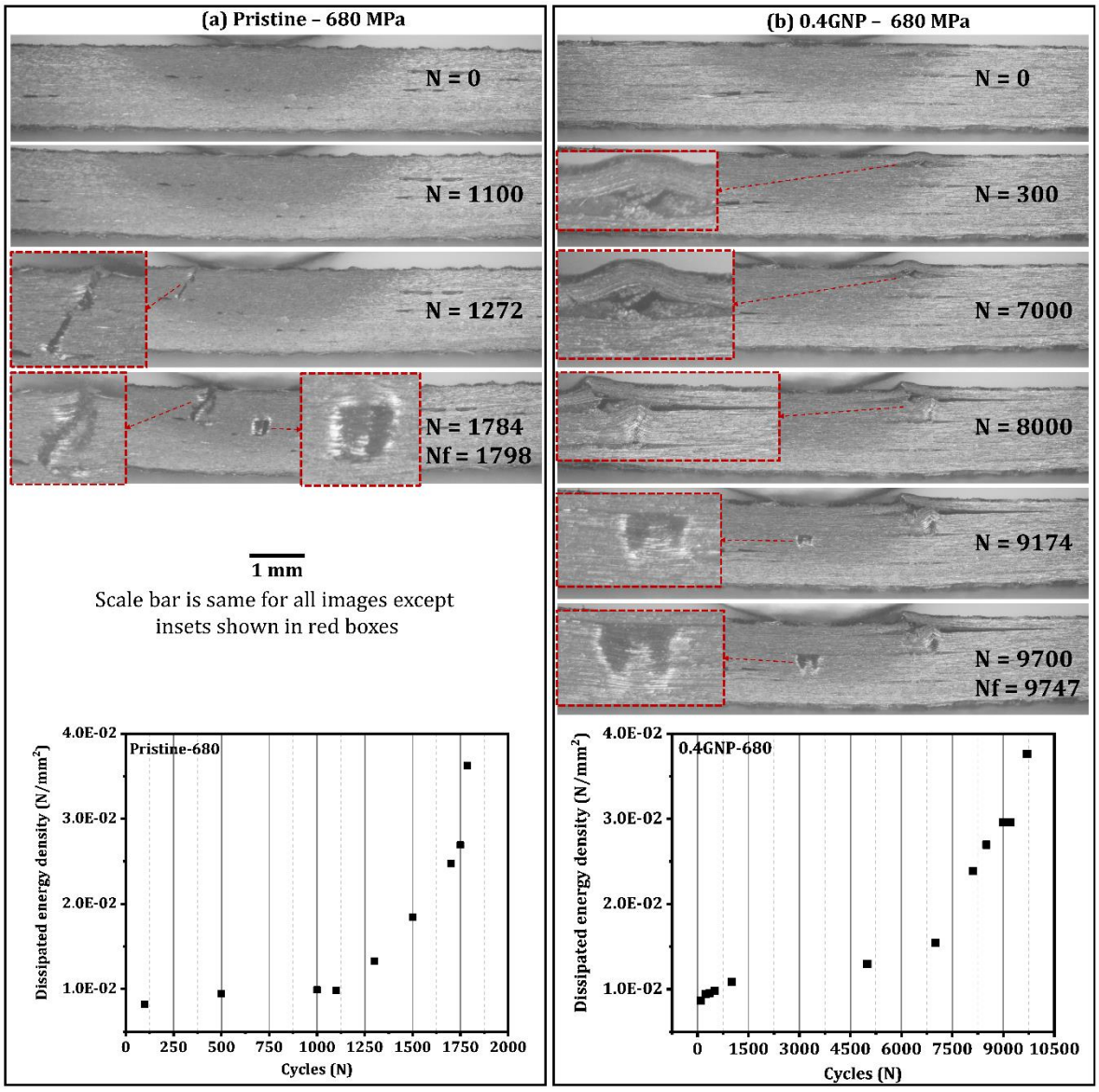

Fig. 6. Progressive damage evolution of GNP/CF/epoxy laminates under flexural fatigue loading at highest stress level (680 MPa) along with respective dissipated strain energy density (DSED) vs number of cycles plot; N – cycles, Nf – cycles to fail

When subjected to a stress level of 640 MPa, pristine specimen undergoes compression-induced deformation under the loading ram after 8500 cycles (Fig. 7a). However, there is a consistent rise in DSED from the beginning until 25000 cycles, followed by a sudden surge

after 25000 cycles. The final micrograph was captured after complete failure of pristine laminate, revealing the failure of entire ply throughout its thickness after 28702 cycles.

In contrast, 0.4GNP specimen subjected to a stress level of 640 MPa exhibited no signs of crack or delamination until 74000 cycles (Fig. 7b). Moreover, there was only a minimal rise in DSED as it approached 74000 cycles. At 74000 cycles, first ply delamination occurred at the top ply of the specimen, but it didn't propagate significantly until 85000 cycles. Associated DSED with the initial ply delamination didn't show a substantial increase between 70000 cycles and 80000 cycles. As the cycles progressed, another ply below the top ply experienced delamination, leading to a sudden surge in DSED. This increase happened more rapidly within a shorter number of cycles, concurrent with the formation of another deformation region beneath the loading ram's center. The deformation region expanded rapidly and the ultimate failure of 0.4GNP laminate occurred after 85510 cycles.

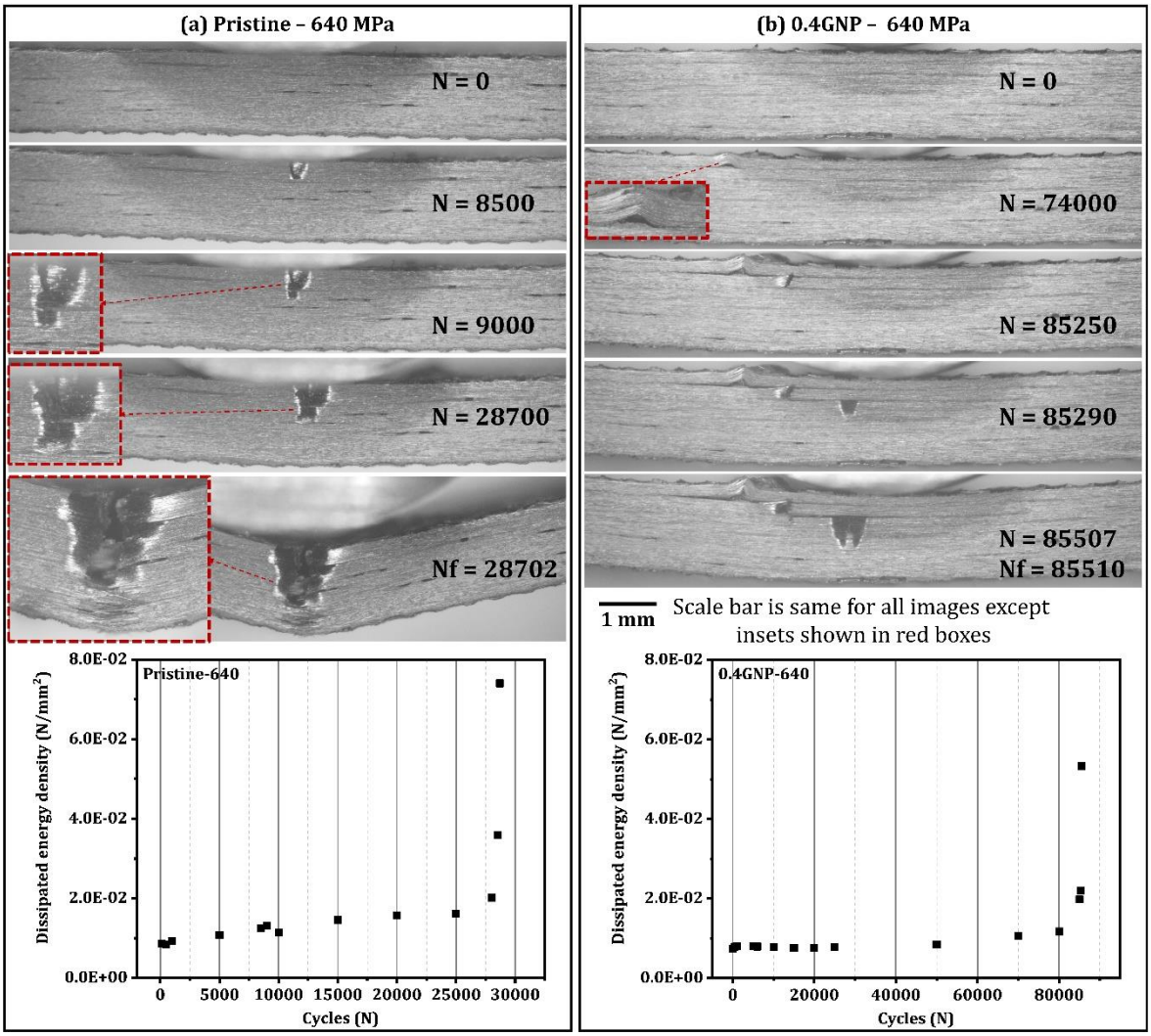

Fig. 7. Progressive damage evolution of GNP/CF/epoxy laminates under flexural fatigue loading at lowest stress levels (640 MPa) along with respective strain dissipated strain energy density (DSED) vs number of cycles plot; N – cycles, Nf – cycles to fail

When subjected to a stress level of 600 MPa, pristine specimen exhibited only a minor increase in DSED despite the formation of a minor delamination of the top ply beneath the loading ram (Fig. 8a). This minor delamination, characterized by the presence of kink bands without propagation, is clearly visible in the insets at 3500 cycles and 50000 cycles.

The DSED did not increase substantially until 185000 cycles. However, at 187700 cycles, another minor delamination occurred which was connected to another bottom ply failure. Subsequently, there was a rapid surge in DSED, ultimately leading to final fracture at 189763 cycles.

Similar to pristine specimen, the initial minor delamination in 0.4GNP specimen did not cause a significant increase in DSED after 80000 cycles (Fig. 8b). This delamination propagated slowly until 650000 cycles and resulted in a decrease in DSED. This decrease in DSED took place after four times as many cycles as in the pristine specimen. Afterwards, a small increase in DSED was observed when another delamination was observed beneath the initially delaminated ply after 686000 cycles. Subsequently, DSED gradually increased while the delamination propagated slowly until 796400 cycles. After that, specimen experienced major ply fracture and delamination in different regions, resulting in a rapid surge in DSED.

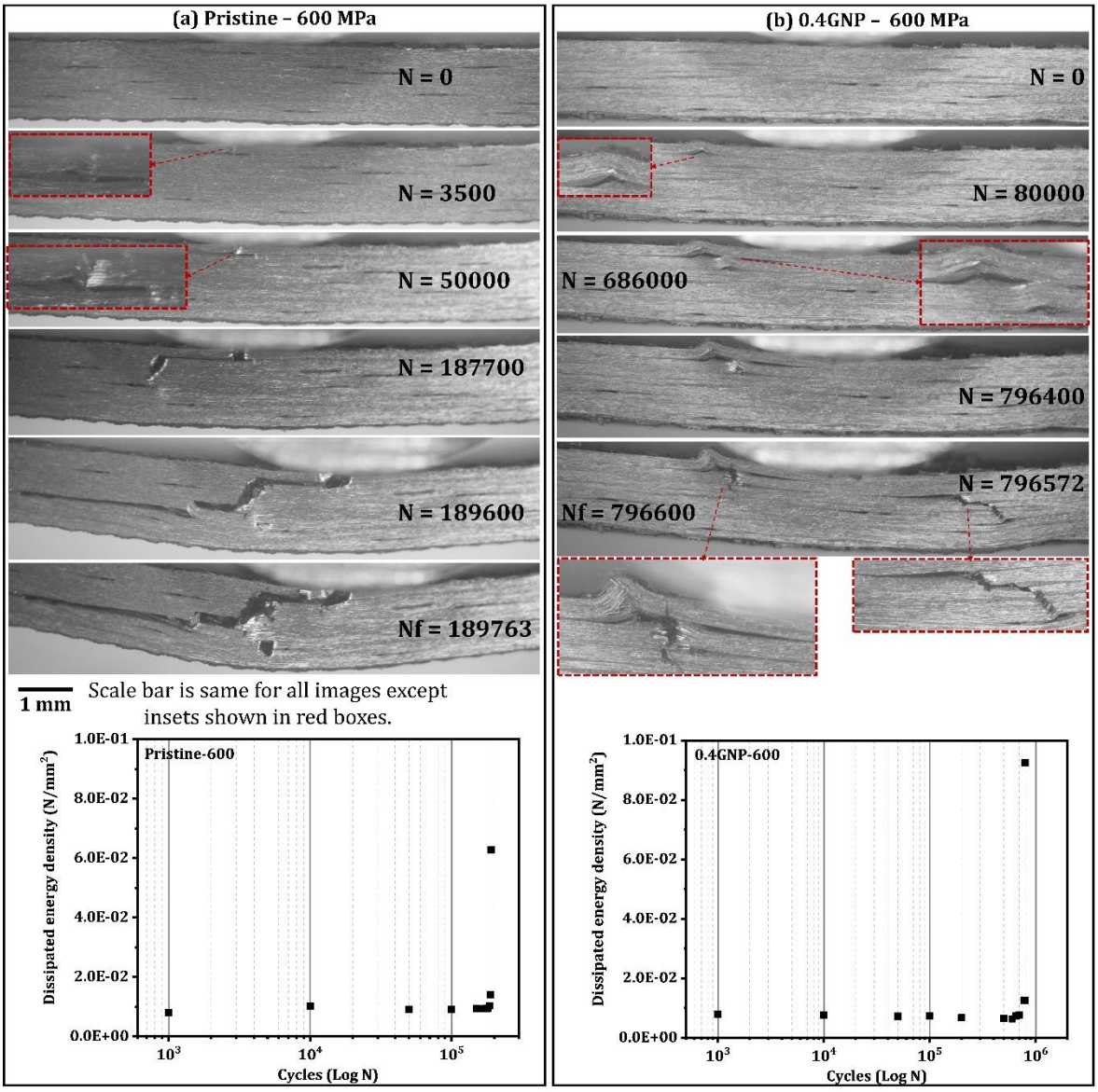

Fig. 8. Progressive damage evolution of GNP/CF/epoxy laminates under flexural fatigue loading at lowest stress levels (600 MPa) along with respective dissipated strain energy density (DSED) vs number of cycles plot; N – cycles, Nf – cycles to fail

At a stress level of 580 MPa, the behavior of both pristine laminate and 0.4GNP laminate differs from the other stress levels. In Fig. 9a and b, it can be observed that both laminates experience a decrease in DSED as the number of cycles increases. Notably, the pristine

laminate demonstrates no crack initiation throughout the entire bending fatigue life cycle, which meets the run-out criteria of 1000000 cycles (Fig. 9a). Similarly, 0.4GNP specimen remains free from cracks or deformations until reaching 278000 cycles at the stress level of 580 MPa (Fig. 9b). After 330000 cycles, a small deformation occurs directly beneath the loading ram, but it does not propagate until reaching the run-out criteria. Interestingly, there is a consistent decrease in DSED observed throughout entire bending fatigue life cycle for 0.4GNP specimen.

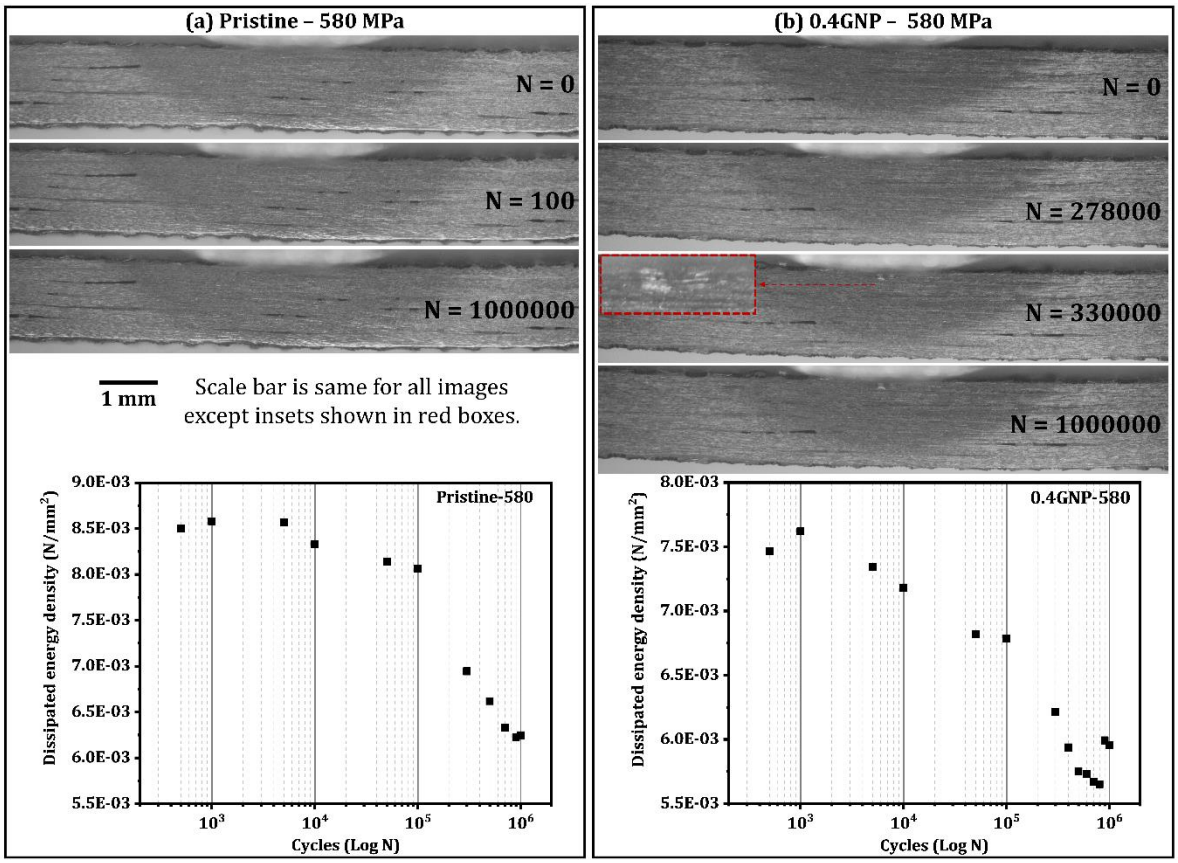

Fig. 9. Progressive damage evolution of GNP/CF/epoxy laminates under flexural fatigue loading at lowest stress levels (580 MPa) along with respective dissipated strain energy density (DSED) vs number of cycles plot; N – cycles, Nf – cycles to fail

3.6 Fracture surface examination

Examination of the transverse cross-section of the failed composites subjected to fatigue loading was done using a scanning electron microscope (SEM) and three distinct regions were observed on the fracture surface (Fig. 10, Fig. 11, Fig. 12 and Fig. 13). The first region, known as the compressive region, was formed due to local compression under the loading ram. The second region, reffered to as the transition region, lies between the compressive and tensile regions. Finally, the third region, known as the tensile region, was formed due to tension at the bottom plies. A representative low magnification micrograph, labeled as (A), is provided for both the pristine and 0.4GNP laminates at all stress levels.

At 680 MPa stress level, fracture surfaces of both pristine and 0.4GNP laminates show flattened epoxy surrounding the carbon fibers in compression regions (Fig. 10a and Fig. 10e respectively). In transition region of pristine laminate (Fig. 10b), there is debris consisting of broken fibers (indicated by white arrows) and epoxy on the fracture surface. Moving towards the bottom, a transitional area can be observed where the fibers, previously covered with epoxy debris, transition into fibers without debris (Fig. 10c). In contrast, fracture surfaces of 0.4GNP laminates show a predominance of epoxy debris throughout most of the region (as observed in Fig. 10f). Furthermore, transitional area depicted in Fig. 10g reveals a distinct transition from a region without any fiber pull-out to a region with evident fiber pull-out (indicated by white circles). In tensile region, Fig. 10 d and Fig. 10 h reveal that 0.4GNP laminate exhibits fewer instances of fiber pull-outs compared to pristine laminate (indicated by white circles).

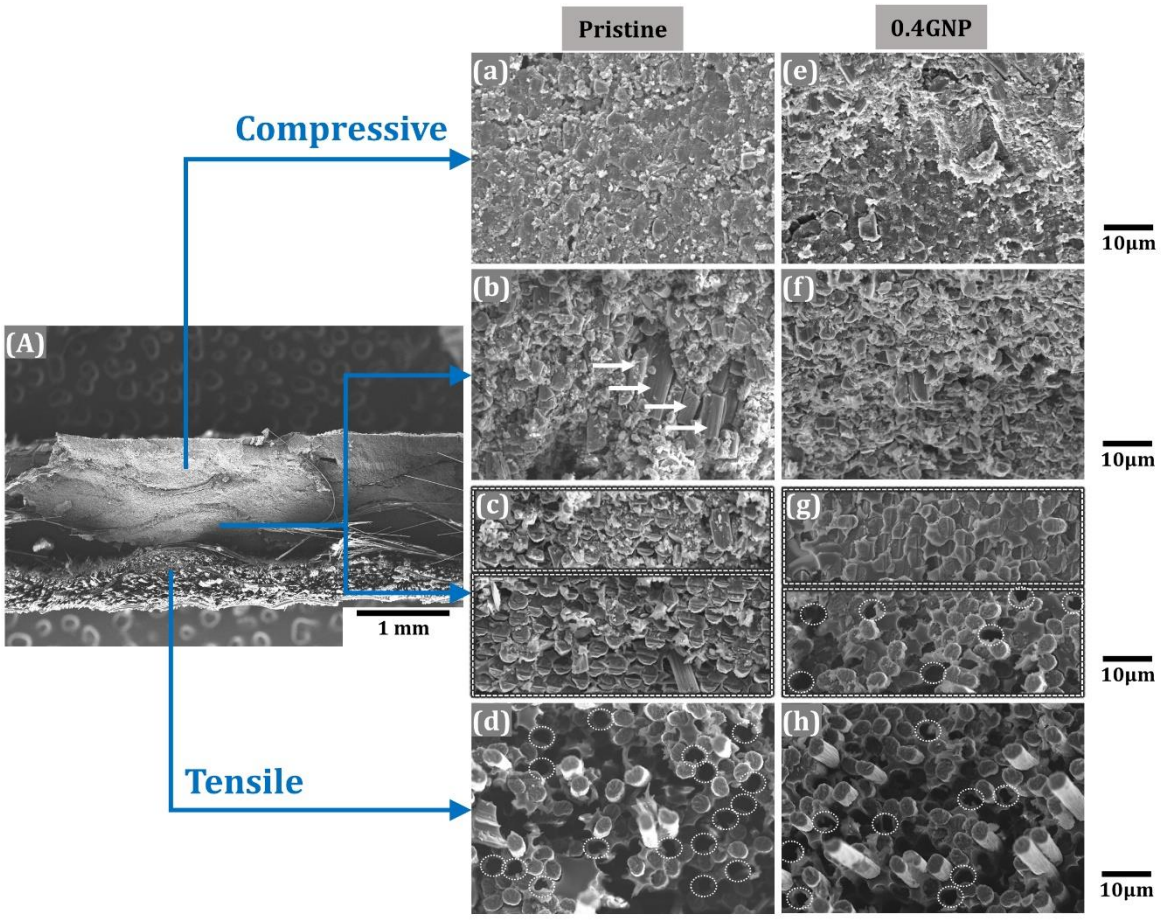

Fig. 10. SEM micrographs of cross-sectional fracture surfaces of speciemens tested under bending fatigue loads at 680 MPa stress level; (A) representative micrograph redirecting the observation region of (a, b c and d) pristine and (e, f, g and h) 0.4GNP laminate

At 640 MPa stress level, fracture surfaces of 0.4GNP laminates exhibit a reduced amount of epoxy debris on the carbon fibers in compression regions compared to pristine laminate (as depicted in Fig. 11e and Fig. 11a, respectively). In the transition regions of pristine laminate (as shown in Fig. 11b), broken fibers and epoxy debris are visible. As we move towards the tensile region, fiber pull-outs can be observed in Fig. 11c and Fig. 11d. However, in the transition region of the 0.4GNP laminate (illustrated in Fig. 11f and Fig.

11g), only epoxy debris is observed except for a small area in Fig. 11f where embedded fibers are visible without any accompanying epoxy debris. In the tensile region of the 0.4GNP laminate, fiber pull-outs are similar to those in the pristine laminates, as shown in Fig. 11h.

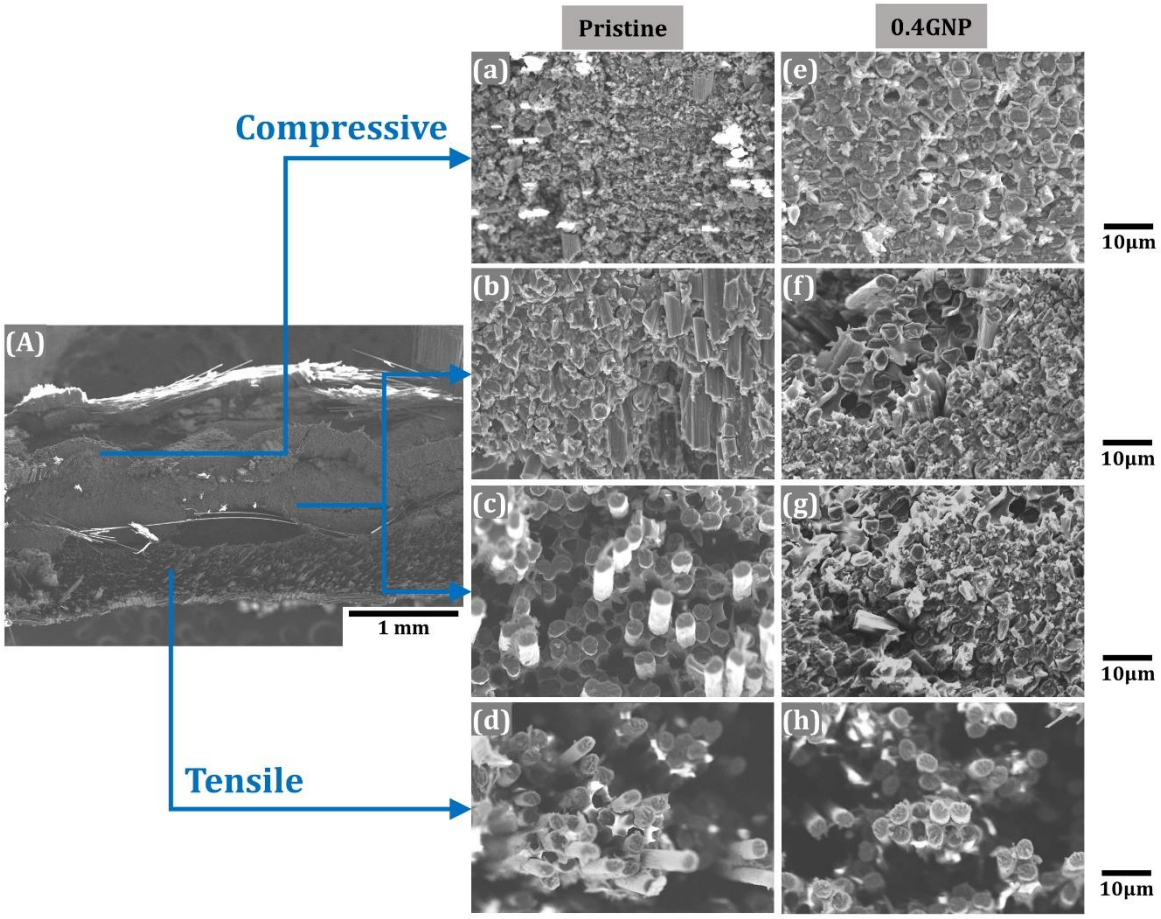

Fig. 11. SEM micrographs of cross-sectional fracture surfaces of speciemens tested under bending fatigue loads at 640 MPa stress level; (A) representative micrograph redirecting the observation region of (a, b c and d) pristine and (e, f, g and h) 0.4GNP laminate

At 600 MPa stress level, fracture surfaces of both pristine and 0.4GNP lamiantes show epoxy debris surrounding the carbon fibers in compression regions (Fig. 12a and Fig. 12e

respectively). In the transition region of both pristine and 0.4GNP laminates, there are minimal differences in the fracture surfaces (as shown in Fig. 12b and Fig. 12f, respectively). However, as we progress towards the tensile region, 0.4GNP laminates exhibit a larger amount of epoxy debris on carbon fibers compared to pristine laminate and the transition is clearly visible in both laminates (depicted in Fig. 12c and Fig. 12g). In the tensile region, pristine laminate displays long fibers protruding from the surface which are clean and free of debris (Fig. 12d). In contrast, 0.4GNP laminate showcases a larger number of fibers strongly adhered to each other, with fewer fiber pull-outs observed (indicated by white circles in Fig. 12h).

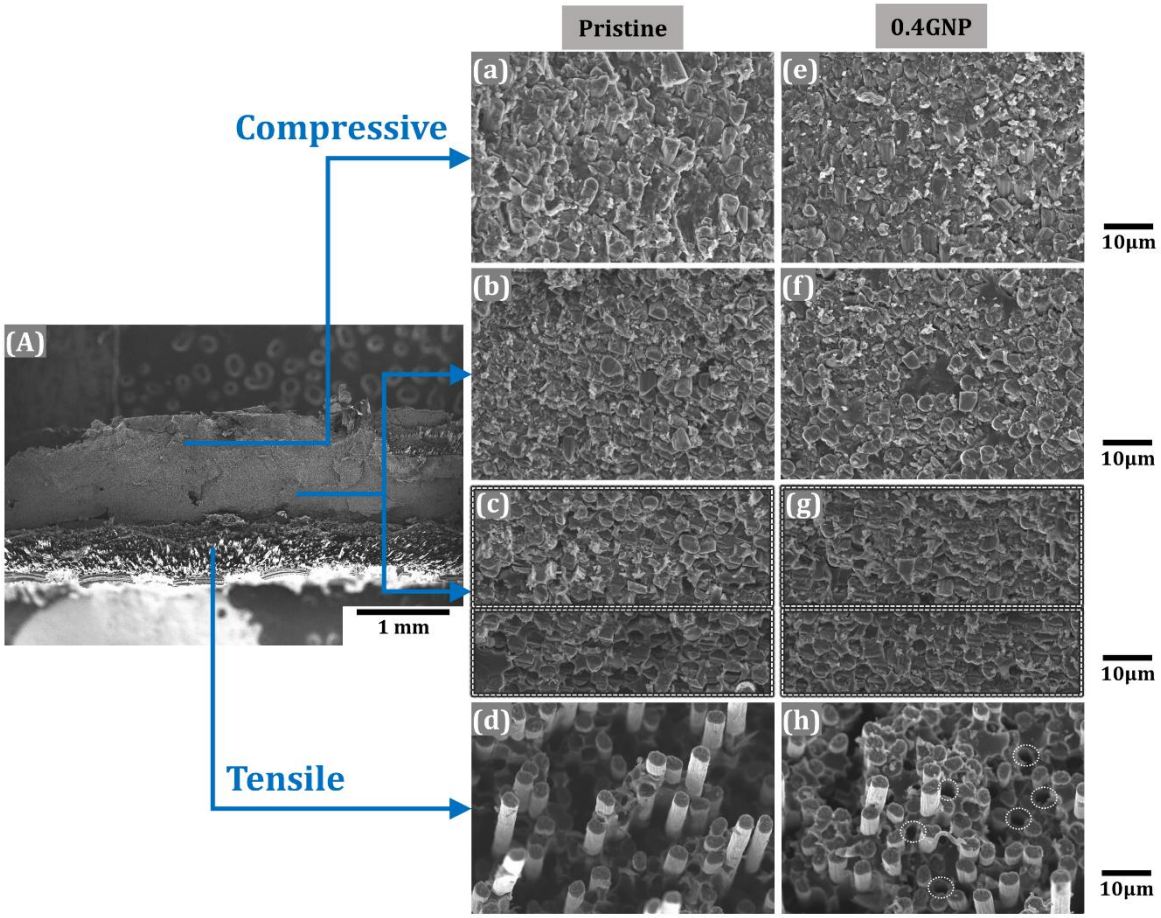

Fig. 12. SEM micrographs of cross-sectional fracture surfaces of speciemens tested under bending fatigue loads at 600 MPa stress level; (A) representative micrograph redirecting the observation region of (a, b c and d) pristine and (e, f, g and h) 0.4GNP laminate

At a stress level of 580 MPa, fracture surfaces of both pristine and 0.4GNP laminates exhibit broken fibers, as indicated by white arrows, along with the presence of epoxy debris (as shown in Fig. 13a and Fig. 13b respectively). However, the number of broken fibers is higher in pristine laminate compared to 0.4GNP laminate. In the transition region of pristine laminate, there is a clear distinction between the compressive region (where epoxy debris is present on the carbon fibers) and the tensile region (where embedded fibers are clearly visible along with fiber pull-outs) (Fig. 13b). On the other hand, 0.4GNP laminate does not show a clear transition, with a few broken fibers present along with epoxy debris (Fig. 13f). As we progress towards the tensile region, 0.4GNP laminate exhibits a lower number of fiber pull-outs, indicated by white circles, compared to the pristine laminate (Fig. 13c, d, g and h).

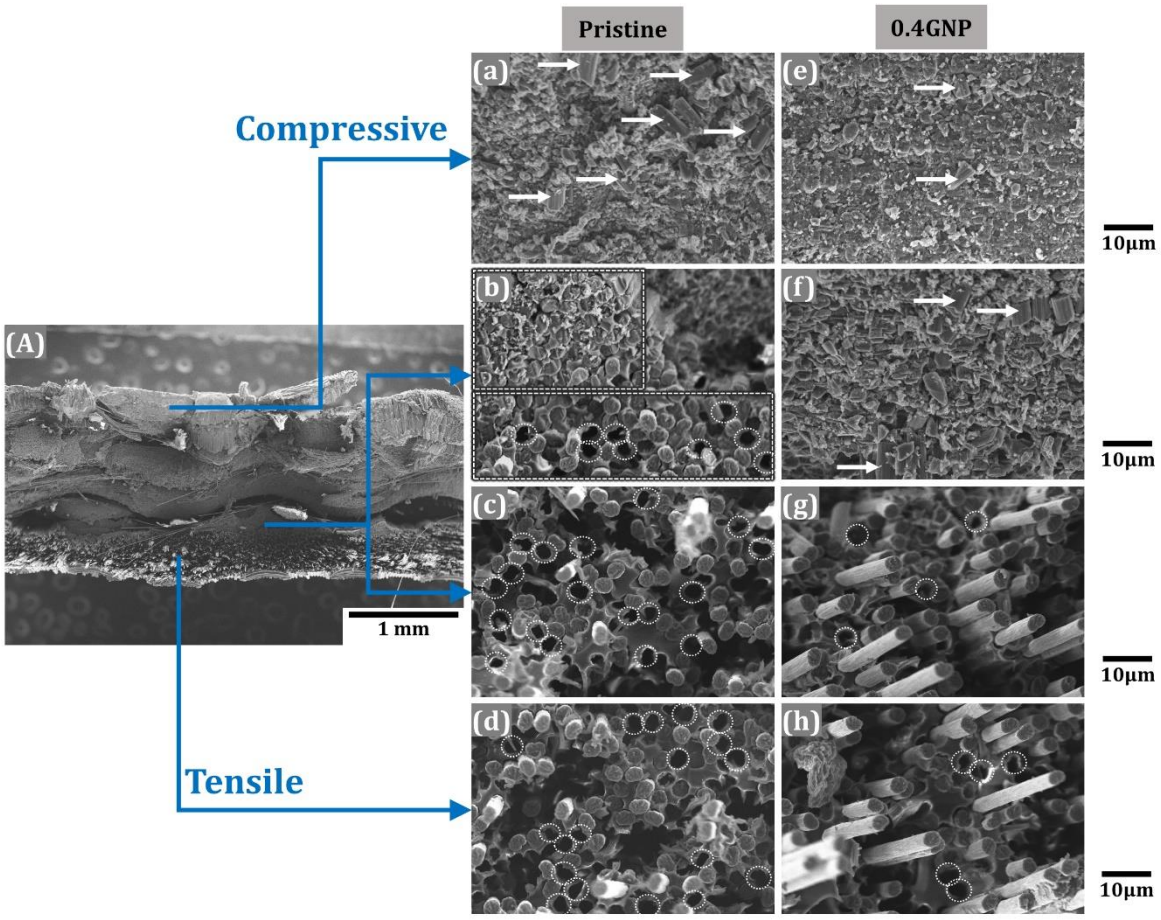

Fig. 13. SEM micrographs of cross-sectional fracture surfaces of speciemens tested under bending fatigue loads at 580 MPa stress level; (A) representative micrograph redirecting the observation region of (a, b c and d) pristine and (e, f, g and h) 0.4GNP laminate

4. Discussion

It has been found that the coating of 0.4 wt.% GNPs on carbon fibers resulted in enhanced uniaxial tensile strength and Young's modulus compared to the pristine laminate. This improvement was attributed to two factors: the formation of a larger interphase region in 0.4GNP laminate and the strong interfacial adhesion between GNPs, carbon fiber and epoxy. Additionally, another study reported the failure of 0.4GNP composites after

sustaining higher localized strains under uniaxial tension, as compared to pristine laminate [12]. In the current study, it is not surprising that the flexural properties of GNP-added laminate showed improvement as well. This improvement can be attributed to the enhanced interfacial adhesion among the graphene nanoplatelets, carbon fiber, and epoxy, similar to the findings in the previous study.

Fatigue failure in CFRPs typically occurs due to the cyclic loading that leads to the initiation of microcracks in the matrix phase. These microcracks then propagate into both the bulk matrix and the interfacial region between fibers and matrix. This process results in matrix cracking, fiber-matrix debonding, delamination, fiber pull-outs and fiber breakage, ultimately causing a loss in the composite's ability to withstand fatigue loading. However, when GNPs are present in the interphase region, they play a beneficial role in mitigating fatigue failure. The presence of GNP diverts and redirects the propagation of cracks in various directions, effectively dispersing the DSED associated with crack propagation [9,22,23]. As a result, GNP-added CFRPs require more cycles to propagate the crack under similar loading conditions.

In pristine laminates, the formation of microcracks is more likely and occurs to a greater extent compared to GNP-added laminates at all stress levels. As a result, the DSED is higher in pristine laminates (Fig. 4 and Fig. 5a, b, c and d). Insitu optical micrographs of progressive damages and the corresponding DSED plots clearly reveal that the rate of increase in DSED is higher in pristine laminate as compared to GNP-added laminate (Fig. 6, Fig. 7, Fig. 8 and Fig. 9). However, at lower stress levels (75-85% of monotonic flexural strength) composites exhibited a reduction in DSED as the cyclic loading advanced (Fig.

5g). This decrease in DSED could potentially be attributed to the phenomena of strain hardening and relaxation of residual stresses. However, strain hardening, which is the increase in strength and hardness associated with plastic deformation, is not a typical characteristic of epoxy under cyclic loading. In CFRPs, epoxy matrix does not undergo plastic yielding due to the presence of brittle fibers and the primary load-carrying responsibility is borne by the fibers themselves. The addition of GNPs to the epoxy matrix does not fundamentally change this behavior.

During cyclic loading, as the material undergoes deformations and stress fluctuations, the relaxation of residual stresses can contribute to DSED within the material. The dissipation of strain energy density can contribute to the overall DSED loss within the material during each loading cycle. However, it is important to note that the relationship between the relaxation of residual stresses and DSED is complex. Factors such as the magnitude and distribution of residual stresses, the loading conditions and the specific microstructure of the CFRP composite can all play a role in determining the extent of DSED. Additionally, other mechanisms such as matrix cracking, fiber-matrix debonding and frictional interactions within the composite can also contribute to DSED during cyclic loading [23]. Thus, relaxation of residual stresses during cyclic loading of CFRPs can contribute to DSED, but it is only one of several factors that influence the overall dissipation of strain energy density within the material. Further information can be found in Appendix A. Additionally, during bending fatigue loading at lower stress levels, plastic strains in the epoxy matrix of carbon fiber reinforced epoxy composites are less likely to occur compared to higher stress levels. At lower stress levels, the epoxy matrix generally exhibits

predominantly elastic and viscoelastic behavior, with minimal plastic deformation. A study by Piyas et al. demonstrated that after unloading, the smaller strain bands experience complete recovery, while the larger bands of strains remain as residue [24]. The irreversible bands may be caused by damage to fibers, matrix and merged pores, whereas the reversible bands are associated with localized elastic stretching. The observed strains in the current work after fatigue loading can arise from limited plastic deformation due to realignment of polymer chains, which enhances the resistance to further deformation.

5. Conclusion

This study aimed to investigate the effect of graphene nanoplatelets (GNP) coating on the flexural and fatigue behavior of GNP/CF/epoxy composites. A thorough analysis of the laminates was conducted using in-situ microscopic examination to observe the initiation and propagation of microcracks during fatigue tests. Furthermore, the fractured surfaces were analyzed using scanning electron microscopy (SEM) to gain insights into the microscopic adhesion between GNP, CF and epoxy. The key results of this study can be summarized as follows:

- The addition of GNPs to CFRPs resulted in enhanced flexural strength and failure strain compared to the pristine CFRPs. A significant improvement of up to 43-fold in fatigue life was observed in the GNP-added composites, particularly at higher stress levels. However, the improvement in fatigue life was less pronounced at lower stress levels.

- Insitu optical micrographs of pristine laminates showed transverse ply failure and epoxy deformation under compression at higher stress levels (680 MPa and 640 MPa). In contrast, GNP-added laminates exhibited initial delamination followed by multiple ply failures after large number of cycles. Both laminates experienced delamination and subsequent ply failures at a stress level of 600 MPa, but the failure was significantly delayed in GNP-added laminates compared to pristine laminates. At the lowest stress level (580 Mpa), neither laminate showed significant cracks or delamination until one million cycles.
- GNP-added laminates demonstrated lower DSED across all stress levels compared to pristine laminates, although this effect was less pronounced at lower stress levels. The observed optical micrographs of crack initiation and progression correlated well with the DSED during the fatigue cycles.
- DSED exhibits an increase with an increasing number of cycles, particularly when subsequent cracks or delaminations are generated, regardless of the stress levels. Furthermore, the occurence of transverse cracks or ply failures results in a higher rate of DSED increase compared to delaminations. However, in the absence of any cracks or delaminations within the laminates, the DSED demonstrates a decrease with an increasing number of cycles, especially at lower stress levels.
- SEM micrographs of the fracture surfaces revealed a clear transition from compression to tensile regions in both laminates. Notably, these micrographs provide evidence of reduced fiber pull-out and improved adhesion among GNP,

carbon fiber and epoxy specifically within the tensile region of the GNP-added laminate.

- Both laminates demonstrated higher residual strength and residual failure strain after one million cycles of loading/unloading. The GNP-added laminate showed superior residual strength and modulus compared to the pristine laminate.

Declarations of interest

The authors have submitted a patent application in India (application number 202321047360) entitled "Enhancing the flexural strength of fiber-composites through cyclical loading." The patent is currently undergoing examination. All authors have confirmed that they do not possess any other conflicts of interest.

Appendix A

A.1 Strain measurement using digital image correlation

Digital image correlation analysis was utilized to measure the strain within both laminates. This measurement was conducted after subjecting the composites to bending cyclic loading at a stress level of 560 MPa, both with and without the addition of GNP. The images of the specimens in their unloaded state were captured when the testing was halted after a specific number of cycles. Fig. A1 illustrates the development of strains in GNP-added composites under lower cyclic stresses, indicating a decrease in DSED. The strain components Exx, Eyy, and Exy represent the axial, transverse and shear directions respectively. In axial direction (Exx), both positive and negative strains randomly appear with an increasing occurrence as the number of cycles increases. The transverse direction exhibits a

compressive region directly beneath the loading ram (center) which does not propagate significantly with increasing cycle count. However, positive strains begin to emerge within the samples after 10,000 cycles. The shear component of strain (Exy) displays clear patterns of both positive and negative strains, which appear to be opposite from the middle of the specimen and progressively increase with each cycle. Thus, there are permanent plastic strains left in the material and this influences the DSED. These strains may be occurring because of stretching of epoxy chains such that future flexural deformation becomes more difficult.

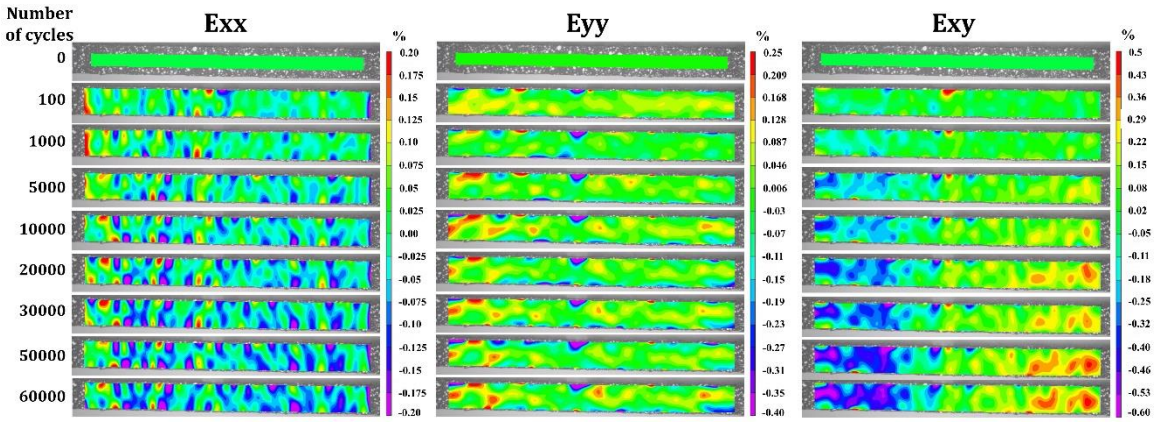

Fig. A1. Strain contours of 0.4GNP composites without any applied load, obtained after subjecting them to cyclic bending at a stress level of 560 MPa

References

[1] Alam P, Mamalis D, Robert C, Floreani C, Brádaigh CMÓ. The fatigue of carbon fi bre reinforced plastics - A review. Compos Part B 2019;166:555–79. https://doi.org/10.1016/j.compositesb.2019.02.016.

[2] Han S, Lin JT, Yamada Y, Chung DDL. Enhancing the thermal conductivity and compressive modulus of carbon fiber polymer-matrix composites in the through-

thickness direction by nanostructuring the interlaminar interface with carbon black. Carbon N Y 2008;46:1060–71. https://doi.org/10.1016/j.carbon.2008.03.023.

[3] Blackman BRK, Kinloch AJ, Sohn Lee J, Taylor AC, Agarwal R, Schueneman G, et al. The fracture and fatigue behaviour of nano-modified epoxy polymers. J Mater Sci 2007;42:7049–51. https://doi.org/10.1007/s10853-007-1768-6.

[4] Kim MT, Rhee KY, Lee JH, Hui D, Lau AKT. Property enhancement of a carbon fiber/epoxy composite by using carbon nanotubes. Compos Part B Eng 2011;42:1257–61. https://doi.org/10.1016/j.compositesb.2011.02.005.

[5] Pathak AK, Borah M, Gupta A, Yokozeki T, Dhakate SR. Improved mechanical properties of carbon fiber/graphene oxide-epoxy hybrid composites. Compos Sci Technol 2016;135:28–38. https://doi.org/10.1016/j.compscitech.2016.09.007.

[6] Xiao L, Ao Y, Zhang M, Liu L, Fu J, Li M. Layer-by-Layer electrostatic self-assembly silica/graphene oxide onto carbon fiber surface for enhance interfacial strength of epoxy composites. Mater Lett 2018;236:69–72. https://doi.org/10.1016/j.matlet.2018.10.077.

[7] Barkoula NM, Alcock B, Cabrera NO, Peijs T. Flame-Retardancy Properties of Intumescent Ammonium Poly(Phosphate) and Mineral Filler Magnesium Hydroxide in Combination with Graphene. Polym Polym Compos 2008;16:101–13. https://doi.org/10.1002/pc.

[8] Wang C, Li J, Sun S, Li X, Zhao F, Jiang B, et al. Electrophoretic deposition of graphene oxide on continuous carbon fibers for reinforcement of both tensile and interfacial strength. Compos Sci Technol 2016;135:46–53. https://doi.org/10.1016/j.compscitech.2016.07.009.

[9] Hung P, Lau K, Fox B, Hameed N, Jia B. Effect of graphene oxide concentration on the flexural properties of CFRP at low temperature. Carbon N Y 2019;152:556–64. https://doi.org/10.1016/j.carbon.2019.06.032.

[10] Han X, Zhao Y, Sun JM, Li Y, Zhang JD, Hao Y. Effect of graphene oxide addition

on the interlaminar shear property of carbon fiber-reinforced epoxy composites. Xinxing Tan Cailiao/New Carbon Mater 2017;32:48–55. https://doi.org/10.1016/S1872-5805(17)60107-0.

[11] Srivastava AK, Singh A. Effect of Graphene Coating of Carbon Fibers on the Fracture of Uni-directional Laminates. Procedia Struct Integr 2022;41:241–7. https://doi.org/10.1016/j.prostr.2022.05.027.

[12] Srivastava AK, Singh A. An investigation on the effect of GNP addition on the mechanism of deformation in unidirectional carbon-fiber epoxy composites using mechanical testing and in-situ SEM. Mater Today Commun 2022;33:104984. https://doi.org/10.1016/j.mtcomm.2022.104984.

[13] Srivastava AK, Gupta V, Yerramalli CS, Singh A. Flexural strength enhancement in carbon-fiber epoxy composites through graphene nano-platelets coating on fibers. Compos Part B Eng 2019;179:107539. https://doi.org/10.1016/j.compositesb.2019.107539.

[14] Srivastava AK, Gupta V, Yerramalli CS, Singh A. Mechanical properties of graphene nano-platelets coated carbon fiber epoxy composites. ICCM Int. Conf. Compos. Mater., Engineers Australia; 2019, p. 163–71. https://search.informit.org/doi/10.3316/informit.854923691619657.

[15] Mishra K, Bastola KP, Singh RP, Vaidyanathan R. Effect of graphene oxide on the interlaminar fracture toughness of carbon fiber/epoxy composites. Polym Eng Sci 2019;59:1199–208. https://doi.org/10.1002/pen.25100.

[16] Srivastava AK, Desai U, Singh A. Effect of graphene coating on modified and pristine carbon fibers on the tribological response of carbon fiber epoxy composites. Compos Part B Eng 2023;250:110412. https://doi.org/10.1016/j.compositesb.2022.110412.

[17] Tareq MS, Jony B, Zainuddin S, Al Ahsan M, Hosur M V. Fatigue analysis and fracture toughness of graphene reinforced carbon fibre polymer composites. Fatigue

Fract Eng Mater Struct 2021;44:461–74. https://doi.org/10.1111/ffe.13371.

[18] Jen YM, Ni WL. Effect of Dispersing Multiwalled Carbon Nanotubes and Graphene Nanoplatelets Hybrids in the Matrix on the Flexural Fatigue Properties of Carbon/Epoxy Composites. Polymers (Basel) 2022;14. https://doi.org/10.3390/polym14050918.

[19] Shen MY, Chang TY, Hsieh TH, Li YL, Chiang CL, Yang H, et al. Mechanical properties and tensile fatigue of graphene nanoplatelets reinforced polymer nanocomposites. J Nanomater 2013. https://doi.org/10.1155/2013/565401.

[20] Knoll JB, Riecken BT, Kosmann N, Chandrasekaran S, Schulte K, Fiedler B. Composites : Part A The effect of carbon nanoparticles on the fatigue performance of carbon fibre reinforced epoxy. Compos PART A 2014;67:233–40. https://doi.org/10.1016/j.compositesa.2014.08.022.

[21] Srivastava AK, Desai U, Singh A. Effect of graphene coating on modified and pristine carbon fibers on the tribological response of carbon fiber epoxy composites. Compos Part B 2023;250:110412. https://doi.org/10.1016/j.compositesb.2022.110412.

[22] Garg AC. Failure Mechanisms in Toughened Epoxy Resins Review A 2006;31:179–223. https://doi.org/10.1016/0266-3538(88)90009-7.

[23] Dassios KG. A review of the pull-out mechanism in the fracture of brittle-matrix fibre-reinforced composites. Adv Compos Lett 2007;16:17–24. https://doi.org/10.1177/096369350701600102.

[24] Chowdhury P, Sehitoglu H, Rateick R. Damage tolerance of carbon-carbon composites in aerospace application. Carbon N Y 2018;126:382–93. https://doi.org/10.1016/j.carbon.2017.10.019.